Supporting Information

The Role of Pore Geometry in Single Nanoparticle Detection

Matthew Davenport[1,2], Ken Healy[2,3], Matthew Pevarnik[2], Nick Teslich[1], Stefano Cabrini[4], Alan P. Morrison[3], Zuzanna S. Siwy[2] and Sonia E. Létant[1]

[1] Physical and Life Sciences, Lawrence Livermore National Laboratory, 7000 East Ave. Livermore, CA 94550
[2] Department of Physics and Astronomy, University of California, Irvine, 4129H Frederick Reines Hall Irvine, CA 92697-4575
[3] Department of Electrical and Electronic Engineering, University College Cork, Ireland
[4] Molecular Foundry, Lawrence Berkeley National Laboratory, 1 Cyclotron Rd., Berkeley, California 94720

Collisions, Long Events and Normal Translocation

A majority of the events observed can be described by what we have labeled "normal translocation": a particle moves through the pore under the influence of the applied electric field causing a single transient dip in the ionic current. However, that is not to say events that did not fall into this category could be viewed as insignificant. These types of events could be separated into two categories: shallow events and long-type events. The former case occurs when a particle approaches the pore lumen, but does not translocate through it; long-type events observed have been attributed to multiple particles translocating through the pore.[1]

Because the particle does not move through the pore in a shallow event, the word "collision" is often used to describe this type of event. An example of a collision is shown in Figure S1(a). These shallow dips were typically seen at low voltages, *i.e.* less than ~100 mV. At higher voltages, it seems the force generated by the electric field is sufficient to overcome the interactions responsible for frustrating translocation (these could be electrostatic in nature as well; recall that both the pore and particle are negatively charged and the pore would exert a repulsive force on the particle).

It is important to remember that several hundred to thousands of events are recorded for each experiment. This means that collisions must make up a significant portion of the observed events to be

detected. Figure S1(b) shows an example of the histogram from an experiment where this is the case. As discussed in the main text, there is a distribution of events and without looking at the resulting histograms, there is no way to ascertain that a shallow event is a collision rather than a low-level normal event. As shown in S1(b), when collisions are significant, they form a distinct distribution shallower than the normal events and can be easily omitted from analysis. While there are likely to be some real events included and some collisions included, again, because of the large number of events gathered, these types of errors are viewed as insignificant. Similarly, in experiments performed at voltages ≥ 100 mV, there are likely to be collision-type events, but their number is negligible compared to the normal type events.

Similarly, long-type events are a concern only when they represent a non-negligible fraction of the total events, so it is important to identify experiments where this is the case. Three examples of long-type events are shown in Figure S1(c). A characteristic feature of long-type events is, after the initial decrease representing an event start, the ionic current increases (above the level of random fluctuations in the ionic current) before decreasing again. This increase/decrease pattern can occur multiple times during one long-type events. As mentioned previously, one cause of this is threading of a string of particles through the pore. For example, in the event labeled 2 in Figure S1(c), there may be an agglomeration of at least three particles with the upward current spikes representing when the next successive particle enters the pore. In the events labeled 1 and 2, successive events are less distinguishable. Another possible cause of these long events is that a single particle dwells within the pore due to a small difference in zeta potentials, ζ_{pore} and $\zeta_{particle}$. Referring to Eq. 14 in the text, a particle's velocity will be related to that difference, $|\zeta_{pore}|-|\zeta_{particle}|$, so a small velocity or long translocation time could simply be the result of a poorly defined difference. Indeed, calculating that difference for long events often returns values less than 1 mV. This is compounded by the fact that zeta potentials of silicon nitride surfaces have been observed to vary over time.[2-3] Ultimately, this

means that ($|\zeta_{pore}|$ - $|\zeta_{particle}|$) can be difficult to define by a single value in our system, making the results of these experiments ambiguous at best.

The challenge is then to identify the experiments where this issue is non-negligible. Because the event duration, or Δt, distributions decay exponentially for times greater than the most probable duration, we cannot simply exclude events with a large Δt values. Put another way, every experiment will have large Δt values compared to the most probable event duration. However, experiments that possess a significant number of long events were found to have large τ values, that is, the exponential decay of the Δt distributions was slow compared to experiments dominated by normal-type events. In our experiments, the threshold value of τ was found to be around 0.6 ms. In Figure S1(d), we plot several observed τ values *vs.* electric field magnitude – the value of which is a consequence of pore geometry and applied voltage – showing that τ appears to be independent of these parameters as well as particle size (50 nm particle experiments are shown as unfilled circles, while the filled circles represent 100 nm particle experiments). Thus, we interpret large τ as an indicator of a significant number of long-type events and experiments possessing this trait were also omitted from analysis. While we are unable to definitively determine a physical significance to $\tau \approx 0.6$ ms, we note that a large portion of normal-event experiments are characterized by $\tau \sim 0.3$ ms as can be seen in the purple region of S1(d). This factor-of-two relation between the τs may be indicative of the onset of multiple particle translocations in our experiments.

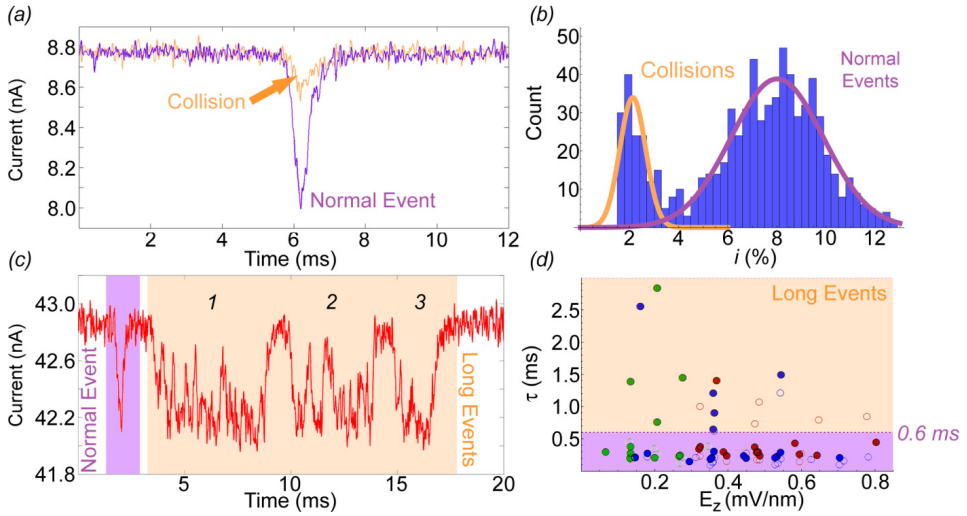

Figure S1: This figure is presented to demonstrate "non-normal" events. In (a), two events from an experiment using 100 nm particles in a 100 nm long, 215 nm diameter pore at 50 mV are overlayed. The deeper of the two is a normal event while the shallower has been identified as a collision. The identification is possible from an analysis of (b), which shows two distinct populations: collisions with a peak near i = 2% and normal events with a peak near i = 8%. The other type of non-normal event, the long event, is shown in (c). This current trace is from 50 nm particles translocating through a 50 nm long, 199 nm diameter pore at 200 mV. It is easiest to identify experiments where long-events are significant by their τ value (which comes from fitting the histograms of event durations with the appropriate probability distribution function). τ is plotted in (d) where values > 0.6 ms usually indicate long-events are an issue and below which, experiments are predominantly populated by normal events.

Bead Mixtures

As the reader may have noted, each histogram has been shown for one bead size measured separately from the other. While these histograms clearly imply that a single pore should be able to differentiate silica particles based on their size, we decided to experimentally verify this implication: for a nanopore sensor to accurately identify the size and geometry of an unknown particle, a known "standard" particle whose diameter is equal to the length of the membrane should be included in the

suspension to identify the β value for the unknown particle. In the absence of standard particle, it may be possible to accurately address unknown particles by incorporating multiple single-pore membranes into the same detector and analyzing the event characteristics from each individual pore; however, our current experimental set-up does not yet allow for this configuration. Figure S2 shows scatter plots for suspensions containing a mixture of 50 nm and 100 nm particles in each membrane thickness at comparable E_z values, flanked by the histograms for event depth and event duration. Bead mixtures present an additional challenge in that one must acquire N times more events compared to a monodisperse sample, where N is the number of different bead sizes present in the same sample (assuming that the total bead concentration is equivalent in the two cases), to build a statistically meaningful histogram for all N species.

As an example of this, compare the event duration histograms for the L_{500} pore to the L_{50} and L_{100} pores. In the latter two cases, one can discern two peaks, whereas only one appears in the L_{500} pore. By sorting events according to event depth, we can break the event duration histograms into two distributions – both of which are described by lognormal and inverse Gaussians as described in the main text of the manuscript as shown in the light purple insets of Figure S2. From this analysis, we can see that there are indeed two separate Δt_{mp} values for the 500-nm long pore as well, yet the relatively low count number for the smaller beads make these indistinguishable when the mixture is viewed as a whole. The fact that we can utilize this post-processing technique based on event depth certainly minimizes this concern as we are still able to obtain the parameters of interest from the PDF fittings.

Returning to the earlier idea of a "standard" particle size, we can test this notion by assuming one of the particle sizes is known and using it to calculate the size of the other particle. As a pivotal role of the standard would be to provide an estimate for which β to use for the unknown particle, the particle whose diameter is closest to the membrane thickness is treated as the standard. The results of this exercise are shown in Table 2 and the agreement is, generally speaking, quite good as all but one of

the d_u values fall within one standard deviation of the mean obtained from SEM sizing (refer to Figure 2d). Recall that the values of β were obtained from studies which examined cases where L >> d or L ≤ d, thus it is not altogether surprising that our intermediate case of the L_{500} pore deviates the most. However, it is worth noting that this deviation is less than 5 nm outside one standard deviation from the mean particle size determined for the d_{50} particles by SEM (which was 57 ± 11 nm). Similarly, treating the zeta potential measured with ELS for the standard particle as a known quantity, we are able to determine values for the zeta potential of the pore and unknown particle which are consistent with values measured in the previous section, with all the ζ_u values falling within the uncertainty measured earlier and all but the 202 nm diameter, 50 nm long pore returning ζ_{pore} values within the range determined previously.

Table S1: Using Nanopores as "Unknown" Particle Analyzers. Results from treating one particle's diameter and zeta potential as a known standard, d_s and ζ_s, respectively, and using these to calculate "unknown" properties of the system, which are subscripted with a "u" in the table. By using the particle with the diameter closest to the membrane thickness, we can identify whether the unknown bead is larger or smaller than the membrane and use the appropriate β and form of Eq. 11 to obtain d_u. Eq 14 can be used with ζ_s to calculate ζ_{pore}, which can then be used to determine ζ_u.

L (nm)	D (nm)	d_s (nm)	β_u	d_u (nm)	ζ_s (mv)	ζ_{pore} (mv)	ζ_u (mv)
50	202	57	1	104 ± 10	-26	-32 ± 4	-29 ± 4
50	252	57	1	92 ± 2	-26	-34 ± 2	-30 ± 1
50	328	57	1	111 ± 6	-26	-38 ± 3	-32 ± 2
100	224	101	3/2	56 ± 1	-34	-41 ± 3	-31 ± 3
100	226	101	3/2	60 ± 3	-34	-40 ± 1	-31 ± 1
100	234	101	3/2	55 ± 1	-34	-39 ± 2	-29 ± 1
500	307	101	3/2	71 ± 3	-34	-49 ± 2	-26 ± 1

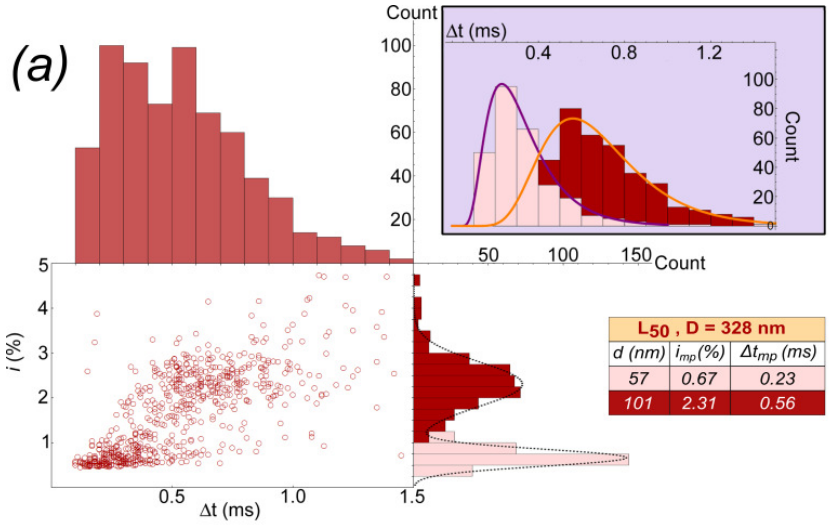
(a)
Count
Δt (ms)
i (%)
Δt (ms)
Count
L50 , D = 328 nm
d (nm) | imp(%) | Δtmp (ms)
57 | 0.67 | 0.23
101 | 2.31 | 0.56

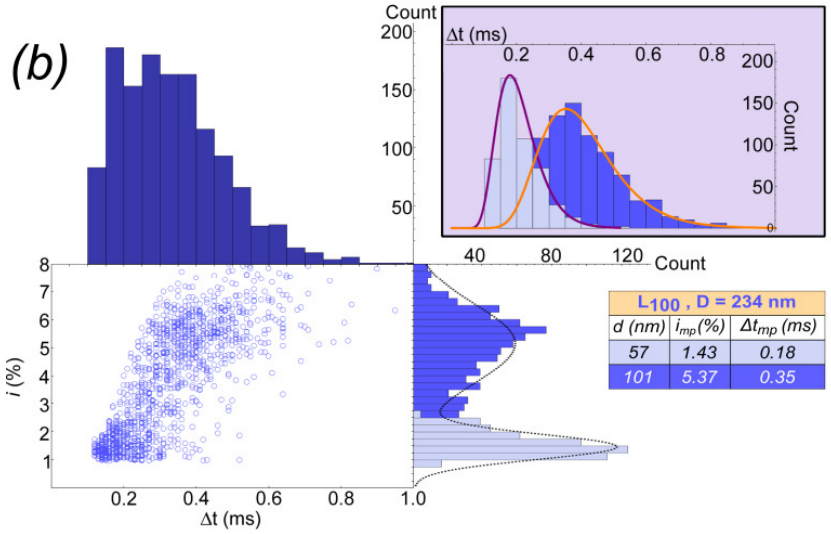
(b)
Count
Δt (ms)
i (%)
Δt (ms)
Count
L100 , D = 234 nm
d (nm) | imp(%) | Δtmp (ms)
57 | 1.43 | 0.18
101 | 5.37 | 0.35

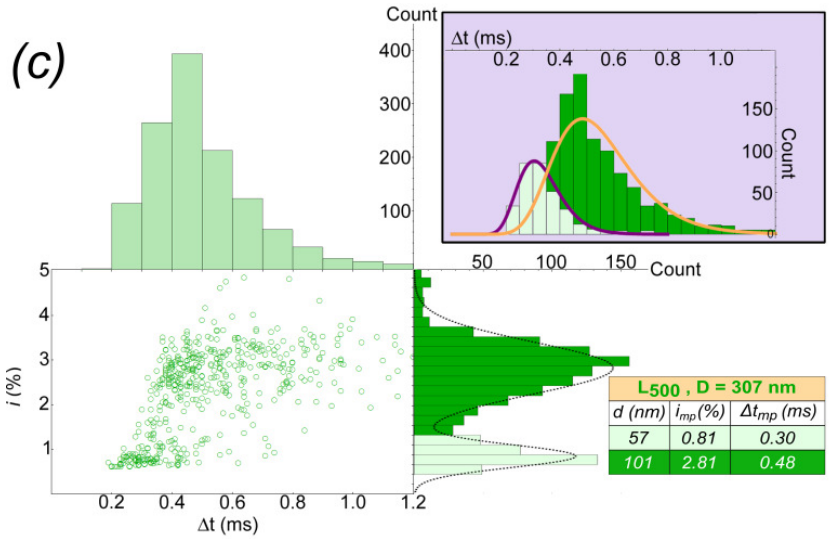
(c)
Count
Δt (ms)
i (%)
Δt (ms)
Count
L500 , D = 307 nm
d (nm) | imp(%) | Δtmp (ms)
57 | 0.81 | 0.30
101 | 2.81 | 0.48

Figure S2: *(a)-(c)* show the results for experiments with mixtures of both particle sizes (50 nm and 100 nm) in L_{50} , L_{100}, and L_{500} membranes respectively. The lower left hand side of each panel plots points according to their amplitude *versus* duration. To the right of this, the histograms for event depth are shown along with a fitting (dashed black line) that is the sum of two Gaussians. From the point of intersection of these Gaussian curves, we can divide the events into two categories: shallow and deep. Above the scatter is the event duration histogram for all events; inset to the right of those are histograms showing event durations after the events are sorted according to depth. The shallow events are fitted with an inverse Gaussian curve (purple) and the deep events are shown with their corresponding lognormal fit (orange). The table is included to show both the mean event depth and most probable event duration (which is the average of the most probable times obtained from both the inverse Gaussian and lognormal fittings).

References

1. Bacri, L.; Oukhaled, A.G.; Schiedt,B.; Patriarche,G.; Bourhis, E.; Gierak, J.; Pelta, J.; Auray, L. Dynamics of Colloids in Single Solid-State Nanopores. *J. Phys. Chem. B*, **2011**, *115*, 2890-2898
2. Bousse, L.; Mostarshed, S. The Zeta Potential of Silicon Nitride Thin Films. *J. Electroanal. Chem.* **1991**, *302*, 269-274
3. Firnkes, M.; Pedone, D.; Knezevic, J.; Döblinger, M.; Rant, U. Electrically Facilitated Translocation of Proteins through Silicon Nitride Nanopores: Conjoint and Competitive Action of Diffusion, Electrophoresis, and Electroosmosis. *NanoLett.* **2010**, *10*, 2162-2167